Structure and Dynamics of Crystal Solvates Hexaphenylditin · 2X, X = Benzene, Toluene, Fluorobenzene, Chlorobenzene, and Aniline. An X-Ray, $P_{(VAPOR)} = f_{(T)}$, and ^2H NMR Study

Karin Eckardt[a], Hartmut Fuess[a], Masakazu Hattori[c], Ryuichi Ikeda[c], Hiroshi Ohki[c], and Alarich Weiss[b]

[a] Fachbereich Materialwissenschaft, Fachgebiet Strukturforschung
[b] Institut für Physikalische Chemie, Technische Hochschule Darmstadt, Petersenstr. 20, D-64287 Darmstadt
[c] Department of Chemistry, University of Tsukuba, Tsukuba, Ibaraki 305, Japan

Z. Naturforsch. **50a**, 758–769 (1995); received March 24, 1995

The crystal structures of the hexaphenylditin (hpdt) solvate compounds, $(C_6H_5)_3Sn-Sn(C_6H_5)_3 \cdot 2X$, solvent X = aniline (an), chlorobenzene (cb), fluorobenzene (fb), and toluene (to), were determined. They are isomorphous with the known benzene (be) crystal solvate compound hpdt · 2be, crystallizing in the trigonal space group $R\bar{3}$, with $Z = 3$ formula units per unit cell. The lattice constants (in pm), from X-ray powder diffraction, are: hpdt · 2an (**1**): $a = 1170.01(9)$, $c = 2641.49(20)$, $c/a = 2.2577$; hpdt · 2be (**2**): $a = 1165.45(5)$, $c = 2641.30(9)$, $c/a = 2.2663$; hpdt · 2cb (**3**): $a = 1175.88(5)$, $c = 2661.66(10)$, $c/a = 2.2635$; hpdt · 2fb (**4**): $a = 1167.69(5)$, $c = 2643.21(9)$, $c/a = 2.2636$; hpdt · 2to (**5**): $a = 1182.24(7)$, $c = 2649.13(11)$, $c/a = 2.2408$. The single crystal structure determination of **5** leads to $a = 1180.2(2)$, $c = 2651.4(5)$. The decomposition of **5** results in the monoclinic phase of hexaphenylditin. Vapor pressure measurements $p = f_{(T)}$, $260 \leq T/K \leq 350$, of the compounds have been performed and the heats of vaporization $\Delta H_v/kJmole^{-1}$ were determined: 52.44 (**1**), 46.65 (**2**), 34.52 (**3**), 43.08 (**4**), 55.30 (**5**). The dynamics of the host molecules C_6D_6, $C_6D_5CD_3$ and $C_6H_5ND_2$ were studied by ^2H NMR in the range $295 \leq T/K \leq 118$. The rotation of the benzene molecule about its threefold axis is maintained till 118 K; in the case of toluene the rotation of the phenyl ring about the pseudo-threefold axis freezes in below 180 K, while the methyl group still rotates about its threefold axis till 123 K.

Introduction

Recently we became interested in molecular solids that form crystal lattices with voids big enough to host molecules from gases or solvents inside. When crystallized from benzene, hexaphenylditin (hpdt), $(C_6H_5)_3Sn-Sn(C_6H_5)_3$, forms a crystal solvate with two benzene molecules per hpdt molecule in the lattice (Krause and Becker [1]). The crystals are not stable, they lose the solvent at atmosphere and become opaque. The crystal structure of hpdt · 2be is known to be trigonal, space group $C_{3i}^2-R\bar{3}$ (Piana et al. [2]). Similar crystal solvates were reported by Toda et al. (1,1,6,6-tetraphenyl-hexa-2,4-diyne-1,6-diol) [3], and by Hart et al. ($Ar_3C-C\equiv C-C\equiv C-CAr_3$) [4], and classified as "wheel-and-axle"-type. Crystal solvates formed by organic molecules are numerous in literature, particularly with CCl_4 as solvent molecule. It seems that the large number of known solids with the composition $A \cdot nCCl_4$ and $A \cdot nC_6H_6$ is due to the frequent use of CCl_4 and C_6H_6 as solvents for recrystallization in chemistry. Their formation is caused by van der Waals interactions and by the principle of optimum space filling within the solid lattice. Today, such crystal solvate compounds are often summarized under the group of inclusion compounds or clathrates, which is quite an unprecise classification.

We wanted to know whether hpdt forms crystal solvates hpdt · nX with other than benzene solvent molecules, whether the inclusion is a question of the shape or size of the guest and whether there is any specific solvent-"mother" molecule interaction. In the following we report on the crystal structures of some hpdt · 2X solvate compounds obtained by X-ray diffraction and by ^2H NMR. Measurements of the vapor pressure of the solvates as a function of temperature give information on the stability of hpdt · 2X and their lattice energy.

Reprint requests to Prof. Al. Weiss.

Experimental

Preparation

Hexaphenylditin was prepared from triphenylchlorotin and sodium in toluene in yields of 40–50%,

0932-0784 / 95 / 0800-0758 $ 06.00 © – Verlag der Zeitschrift für Naturforschung, D-72027 Tübingen

following a method described by Krause and Grosse [5], see also [1]. The solvents X, used for recrystallisation of hpdt and formation of hpdt · 2X were commercial products (Aldrich), purified by fractional crystallization except aniline, which was distilled at 54 °C/40 mbar. The compounds hpdt · 2X were obtained as colourless lustrous rhombohedral crystals by dissolving hpdt in the respective pure liquid solvent and crystallization there from. They were used in the protonated form of X as solvate for the X-ray diffraction experiments as well as for vapor pressure determinations.

Deuterobenzene C_6D_6 and deuterotoluene $C_6D_5CD_3$ were available (Aldrich). $C_6H_5ND_2$ was prepared by refluxing 30 ml of aniline with 10 ml of D_2O for three hours, separating the organic layer and repeating the experiment three times. Finally the organic layer was distilled at 47–52 °C ($p = 39$ mbar), and thus partially deuterated aniline was recovered. The grade of deuteration was determined via high resolution ^1H NMR to be 96% D. Crystallization of hpdt from the deuterated solvents yielded the hpdt · 2X compounds for the ^2H NMR solid state experiments. The crystals were filtered off and sealed in glass tubes under vacuo.

Table 1. Experimental conditions for the crystal structure determination and crystallographic data for hexaphenylditin · 2 toluene, hpdt · 2to (**5**). Diffractometer: CAD-4; wavelength 71.069 pm (MoKα); monochromator: graphite (002); scan: $2\Theta/\omega$. $C_{50}H_{46}Sn_2$; $M = 884.3$.

Crystal size/mm^3	$0.5 \times 0.3 \times 0.2$
Colour	colourless
Temperature/K	301
Absorption coefficient/μm^{-1}	1096
Θ-range for data coll.	$2.14 \leq \Theta \leq 27.96$
Index range	$-15 \leq h \leq 13$ $0 \leq k \leq 15$ $-34 \leq l \leq 34$
Lattice constants/pm	$a = 1180.2(2)$ $c = 2651.4(5)$
$V \cdot 10^{-6}$/(pm^3)	3199.4(8)
space group	$R\bar{3} = C_{3i}^2$
Formula units Z	3
ϱ_{calc}/(Mg · m^{-3})	1.377(1)
F(000)	1338
Reflections collected	5386
Symmetry independent	1721
[R_{int}]	0.0449
Data	1721
Restraints/parameters	2/83
Goodness of fit on F^2	1.094
Final $R(I > 2\sigma(I))$	0.0485
R indices (all data)	$R = 0.0576$, $R_w = 0.1277$
Largest diff: (peak, hole)/ (10^{-6} e(pm)^3)	3.285, −0.391
Max. and min. Transm.	99.95 and 95.39
Extinction coeff.	0.0000(3)
Point positions	Sn in 6c; C, H in 18f

X-ray Diffraction

A single crystal of hpdt · 2 toluene was fixed and sealed in a Lindemann-capillary. Data were collected on a four circle diffractometer CAD-4 at room temperature. From the collected diffraction intensities, after appropriate correction for absorption and Lorentz-polarization factor, the structure was determined by direct methods, Fourier synthesis, and least squares refinement (Sheldrick [6]). Experimental parameters for the structure determination and crystallographic data are given in Table 1.

The X-ray powder diagrams were obtained at room temperature on an X-ray powder diffractometer STOE STADIP, CuKα radiation (156.054 pm), graphite monochromator, in a Debye-Scherrer modus with a position sensitive detector. Reflections were scanned in the range $5 \leq 2\Theta \leq 90°$. For the measurements, the crystals were pulverized under the corresponding solvent and sealed in a capillary with a small amount of solvent to avoid decomposition.

For decomposition experiments, hpdt · 2to was pulverized and filled in an open glass tube, allowing slow evaporation of the solvent during the experiment. Then, a series of X-ray powder diagrams were taken at 50 °C with an interval of 1 hour between each measurement, with the X-ray powder diffractometer mentioned above, using a stationary position sensitive detector.

Vapor Pressures

The vapor pressures of hpdt · 2be (**2**) and hpdt · 2to (**5**) were measured in an apparatus described in short below. The construction is similar to the isoteniskope of Smith and Menzies [7]. The apparatus sketched in Fig. 1 consists of a U-tube (3), that is half filled with a silicon oil. As a safety device for overflowing silicon oil, the U-tube is connected on each side to a trap (2). The sample under investigation is filled into a flask (4), fused on the right side of the U-tube. On the left side, a mercury manometer allows the determination of the pressure with an accuracy of ±0.25 Torr, and the apparatus can be evacuated with the aid of a pump. Temperatures within a range $293 \leq T/K \leq 333$ can be adjusted by a thermostat (5). Stopcocks allow cutting

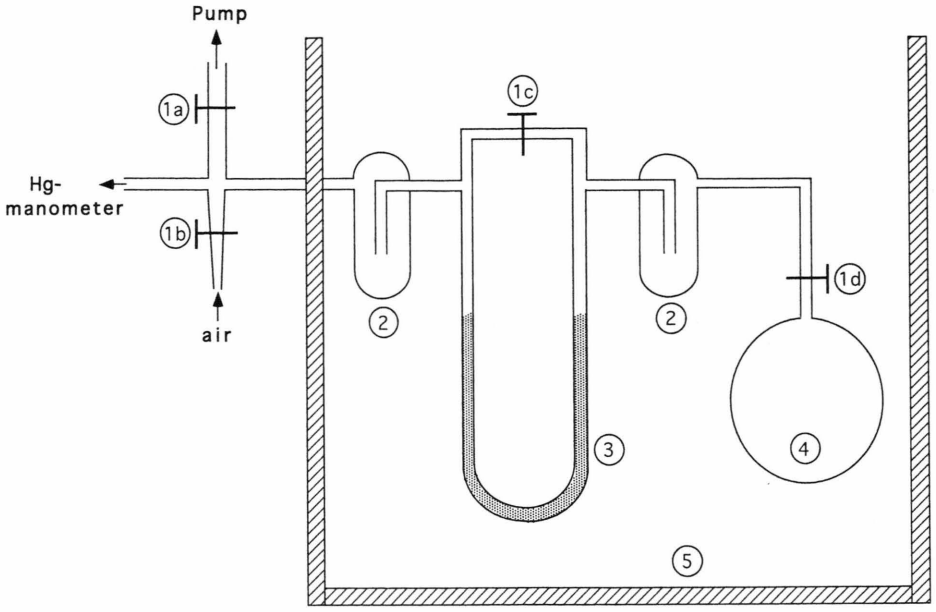

Fig. 1. Sketch of the apparatus used for the vapor pressure measurements. 1a–d: stopcocks; 2: traps; 3: U-tube; 4: sample flask; 5: thermostat.

off different parts of the apparatus. Before each measurement, all stopcocks except (1b) are opened and the apparatus is evacuated cautiously. Then, the flask containing the sample under investigation is cut off by closing (1d), the rest of the apparatus still being evacuated. At $p \leq 0.25$ Torr pressure, valves (1a) and (1c) are closed, the silicon level on the left and right side of the U-tube being equivalent. At a defined temperature T, (1d) is opened, the vapor evolved by the sample increases the pressure on the right side of the U-tube, leading to a decrease of the silicon level on the sample side. This height difference in the U-tube can be compensated by the same pressure on its left side, measuring out a small amount of air by the capillary valve (1b). After some time, when the system is in equilibrium at a given temperature, the final $p_{(T)}$ can be determined from the Hg-manometer.

The vapor pressures of the title compounds **1**, **3**, and **4** were measured in an apparatus consisting of a metal vessel containing the samples, and provided with a pressure transducer for the determination of p. The apparatus can be heated or cooled by the aid of a thermostat. The detailed construction will be described elsewhere (Strauss [8]).

^2H NMR

^{2}H NMR spectra in hpdt · 2X (X = C_6D_6, $C_6D_5CD_3$, $C_6H_5ND_2$) were measured at a Larmor frequency of 46.1 MHz in a temperature range 118–295 K using a Bruker MSL-300 spectrometer equipped with a VT-1000 temperature controller. The quadrupole echo pulse sequence with a 90° pulse width of 6–8 μs was employed (Davis et al. [9], Sternin et al. [10]); spectra were accumulated from 200 to 2000 scans.

Results

Crystal Structure Determinations (X-ray Diffraction)

Hexaphenylditin forms inclusion compounds with toluene, aniline, fluorobenzene and chlorobenzene, analogous to the already known benzene clathrate [2]. The host:guest rates were determined by thermogravimetry to be 1:2. All compounds are stable only in solution or in a saturated atmosphere vessel. From chlorobenzene and fluorobenzene only very dilute solutions give the rhombohedral shaped com-

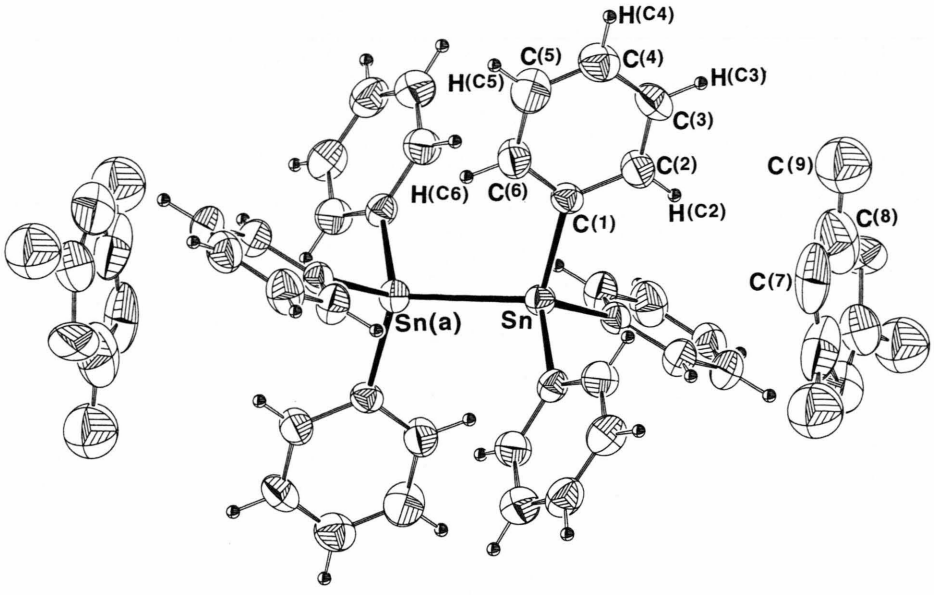

Fig. 2. Molecular structure of hpdt · 2to (thermal ellipsoids at 30% probability level).

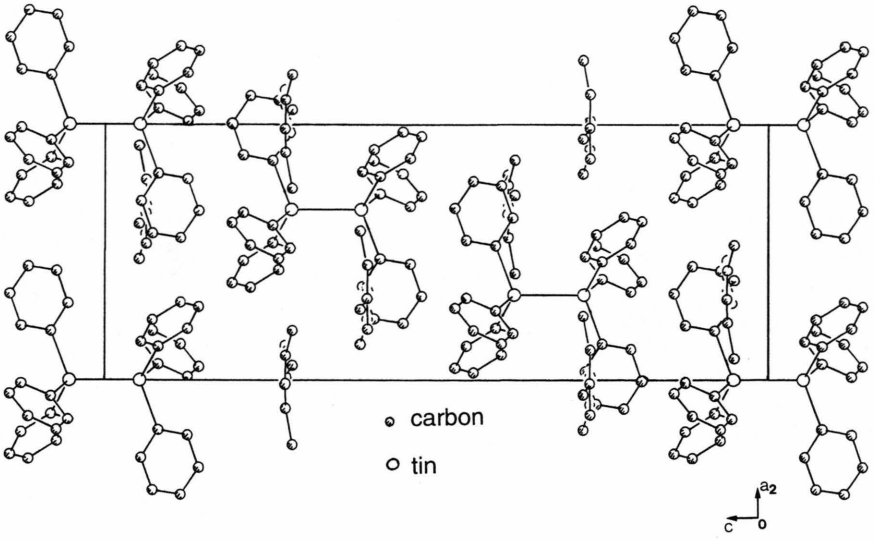

Fig. 3. Projection of the unit cell of hpdt · 2to along [100] onto the ac plane.

pounds; at higher concentrations a mixture of the monoclinic (Preut et al. [11]) and the hexagonal modification is obtained. Crystallization from tetrachloromethane or acetonitrile, or from the aromatic solvents pyridine, benzonitrile, nitrobenzene, p-xylene or mesitylene gave no crystal solvates under the preparation methods applied, although most of these molecules are comparable in size to toluene or chlorobenzene and should fit in the voids.

Single Crystal Structure of hpdt · 2to

The single crystal structure determination of hpdt · 2to leads to the space group $R\bar{3} = C_{3i}^2$ with $Z = 3$

Table 2. Atomic coordinates ($\times 10^4$), isotropic mean thermal parameters [U_{eq}] and thermal parameters U_{ij} for hpdt · 2to (**5**). [U_{eq}] and U_{ij} are given in [pm^2]. The temperature factor takes the form: $T = \exp\{-2\pi^2 (U_{11} h^2 a^{*2} + U_{22} k^2 b^{*2} + U_{33} l^2 c^{*2} + U_{12} hka^* b^* + U_{13} hla^* c^* + U_{23} klb^* c^*)\}$. U_{eq} is defined as 1/3 of the trace of the orthogonalized tensor U_{ij}. For the numbering of the atoms see Figure 2. C(9) is only refined with isotropic temperature factor.

Atom	x/a	y/a	z/c	U_{eq}
Sn	10000	10000	526(1)	553(2)
C(1)	8076(4)	9380(4)	807(1)	598(8)
C(2)	7872(5)	9880(5)	1250(2)	772(11)
C(3)	6614(6)	9481(6)	1420(2)	882(14)
C(4)	5554(5)	8598(6)	1143(2)	846(13)
C(5)	5727(5)	8080(6)	719(2)	891(14)
C(6)	6995(4)	8478(5)	545(2)	762(11)
C(7)	4682(18)	6850(36)	−622(4)	2142(77)
C(8)	4288(25)	7771(22)	−614(4)	2054(64)
C(9)	5268(34)	9181(24)	−511(17)	1806(131)

Atom	U_{11}	U_{22}	U_{33}	U_{12}	U_{13}	U_{23}
Sn	557(2)	557(2)	546(3)	279(1)	0	0
C(1)	620(19)	648(20)	567(18)	348(17)	75(15)	76(15)
C(2)	772(26)	800(27)	712(24)	367(23)	52(20)	−68(20)
C(3)	926(34)	1002(36)	802(30)	544(31)	243(25)	33(26)
C(4)	704(26)	1024(36)	853(30)	465(26)	197(23)	194(26)
C(5)	613(24)	1015(37)	884(31)	287(25)	29(22)	46(27)
C(6)	655(23)	864(28)	665(22)	303(21)	42(18)	−77(21)
C(7)	1930(159)	3635(231)	1040(71)	1525(191)	−63(78)	−473(131)
C(8)	2518(181)	2893(184)	847(57)	1425(131)	91(83)	−169(81)

Table 3. Intramolecular distances (bond distances) d/pm and bond angles (degree) in the molecule hpdt · 2to (**5**). Intermolecular distances within the van der Waals distances ≤380 pm. Data of atoms that are marked with a star * are generated by symmetry.

Connection	d/pm	Connection	angle/degree	Connection	d/pm
Sn–Sn	279.09 (8)	C(1)–Sn–C(1*)	108.62(10)	$H^{(C2)} \cdots H^{(C3)}$	313.7
Sn–C(1)	214.1(4)	C(1)–Sn–Sn*	110.31(10)	$H^{(C3)} \cdots H^{(C3*)}$	344.5
C(1)–C(2)	138.9(6)	Sn–C(1)–C(2)	121.9(3)	$H^{(C4)} \cdots H^{(C4*)}$	318.8
C(2)–C(3)	138.9(7)	Sn–C(1)–C(6)	120.6(3)	$H^{(C3)} \cdots H^{(C4)}$	305.2
C(3)–C(4)	137.3(8)	C(1)–C(2)–C(3)	120.9(5)	$C^{(2)} \cdots H^{(C3)}$	344.5
C(4)–C(5)	134.4(8)	C(2)–C(3)–C(4)	119.9(5)	$C^{(7)} \cdots H^{(C5)}$	314.4
C(5)–C(6)	140.2(7)	C(3)–C(4)–C(5)	120.3(5)	$C^{(8)} \cdots H^{(C5)}$	325.2
C(6)–C(1)	136.9(6)	C(4)–C(5)–C(6)	119.9(5)	$C^{(9)} \cdots H^{(C5)}$	337.8
C(7)–C(8)	138.0(9)	C(5)–C(6)–C(1)	121.5(4)	$C^{(9)} \cdots H^{(C6)}$	359.9
C(7)–C(8*)	138.0(2)	C(6)–C(1)–C(2)	117.5(4)		
C(8)–C(9)	150.3(10)	C(7)–C(8)–C(7*)	140(2)		
		C(8)–C(7)–C(8*)	100(2)		
		C(7)–C(8)–C(9)	120(3)		
		C(9)–C(8)–C(7*)	100(3)		

(hexagonal setting). For lattice constants and further crystallographic data see Table 1. The refined atomic positions and thermal parameters are listed in Table 2. The Sn–Sn-bond of the hpdt molecule is oriented parallel to the threefold axis, and on each side of it one toluene molecule is placed, the toluene ring plane being perpendicular to the 3-fold axis as shown in Figure 2. This conformation is analogous to hpdt · 2be and other similar inclusion compounds [2, 12]. In Table 3 the intramolecular distances and angles are reported, as well as some intermolecular distances. The phenyl rings of hpdt have nearly planar geometry, the calculated best plane and the distances to this plane are referred in Table 4. The toluene ring is distorted and deviates from hexagonal symmetry. Because of the fast thermal motion of the solvent molecule, no hydrogen atoms were fixed for toluene. Despite of this disorder, the C-atoms of the solvent

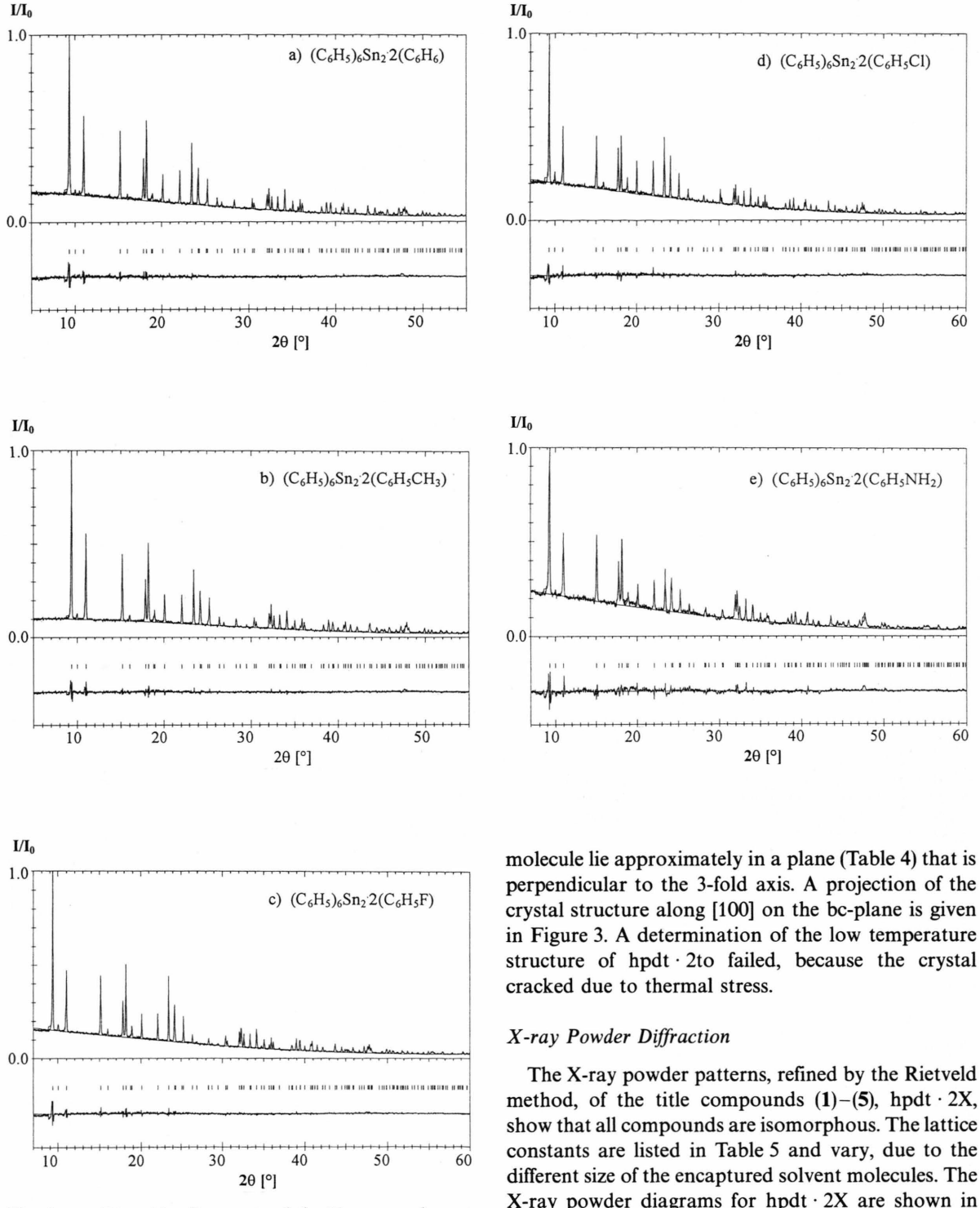

Fig. 4a–e. Rietveld refinements of the X-ray powder patterns of the title compounds (**1**)–(**5**), 1.0 unit corresponds to a) 2306, b) 2492, c) 4137, d) 3002, e) 1831 counts.

molecule lie approximately in a plane (Table 4) that is perpendicular to the 3-fold axis. A projection of the crystal structure along [100] on the bc-plane is given in Figure 3. A determination of the low temperature structure of hpdt · 2to failed, because the crystal cracked due to thermal stress.

X-ray Powder Diffraction

The X-ray powder patterns, refined by the Rietveld method, of the title compounds (**1**)–(**5**), hpdt · 2X, show that all compounds are isomorphous. The lattice constants are listed in Table 5 and vary, due to the different size of the encaptured solvent molecules. The X-ray powder diagrams for hpdt · 2X are shown in Figure 4a–e. To check whether there is a phase transition between the rhombohedral inclusion com-

Table 4. Best planes through the phenyl ring, a), and the toluene ring, b), in (**5**) in hexagonal fractional coordinates; distances d/pm of the carbon atoms from the best planes. The atoms used for the plane calculation are marked with (*), data of atoms generated by symmetry with (′) and (″).

Equations:

a) $-5.009x+10.087y-13.770z=4.303$,
b) $0.028x-0.584y+26.469z=2.015$

a) phenyl ring		b) toluene ring	
Atom	d/pm	Atom	d/pm
C(1)	0.3 *	C(7)	4.3 *
C(2)	−0.1 *	C(7′)	9.6 *
C(3)	−0.7 *	C(7″)	−2.6 *
C(4)	−1.4 *	C(8)	7.7 *
C(5)	−1.2 *	C(8′)	−4.6 *
C(6)	0.3 *	C(8″)	−3.1 *
Sn	5.0	C(9)	−11.3 *

Table 5. Lattice constants of the title compounds from X-ray powder diagrams at room temperature. For comparison, the single crystal (sc) data of (**5**) and (**2**) are given, too.

Compound	*a*/pm	*c*/pm	*c*/a	Remark
hpdt · 2an (**1**)	1170.01(9)	2641.49(20)	2.2577	this paper
hpdt · 2be (**2**)	1165.45(5)	2641.30(9)	2.2663	this paper
hpdt · 2be (**2**)	1152.5	2618.0		[2], sc
hpdt · 2cb (**3**)	1175.88(5)	2661.66(10)	2.2635	this paper
hpdt · 2fb (**4**)	1167.69(5)	2643.21(9)	2.2636	this paper
hpdt · 2to (**5**)	1182.24(7)	2649.13(11)	2.2408	this paper
hpdt · 2to (**5**)	1180.2(2)	2651.4(5)		this paper, sc

Table 6. Results of the vapor pressure measurements. For comparison the numerical data for the pure solvents (liquid state) from literature are given, too. ΔT is the temperature range of the measurement, ΔH_v the heat of vaporization.

a) Equations for the straight lines $\log_{10} p_{(T)}$.

Compound	Equation for the straight line
hpdt · 2an (**1**)	$\log_{10}(p/\text{mbar}) = 9.117-2739.3\ T^{-1}\cdot K$
hpdt · 2be (**2**)	$\log_{10}(p/\text{mbar}) = 9.895-2436.4\ T^{-1}\cdot K$
hpdt · 2cb (**3**)	$\log_{10}(p/\text{mbar}) = 7.396-1803.1\ T^{-1}\cdot K$
hpdt · 2fb (**4**)	$\log_{10}(p/\text{mbar}) = 9.474-2250.4\ T^{-1}\cdot K$
hpdt · 2to (**5**)	$\log_{10}(p/\text{mbar}) = 11.013-2888.9\ T^{-1}\cdot K$

b) Enthalpy ΔH_v/kJmole^{-1} of vaporization

Compound	ΔH_v/kJmole^{-1}	*T*/K	Lit.
hpdt · 2an (**1**)	52.44	295–353	this paper
aniline	52.22		[13]
hpdt · 2be (**2**)	46.65	295–333	this paper
benzene	33.42		[14, 15]
hpdt · 2cb (**3**)	34.52	295–333	this paper
chlorobenzene	39.17		[13, 16]
hpdt · 2fb (**4**)	43.08	260–308	this paper
fluorobenzene	35.76		[16]
hpdt · 2to (**5**)	55.30	295–322	this paper
toluene	37.59		[13]

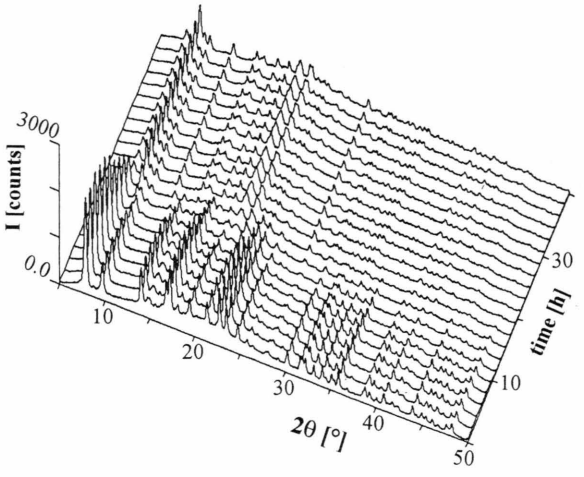

Fig. 5. X-ray powder diagrams taken during the decomposition of the rhombohedral compound hpdt · 2to, to the solvent-free modification of hpdt.

pound and the decomposed one, a series of X-ray powder diagrams were taken during the decomposition of hpdt · 2to. It leads to a diagram that coincides with that of the solvent free modification of hpdt, being monoclinic C_{2h}–$P2_1/c$ [11]. Here, no other phase is formed like with hexaphenyldigermane, where an unstable hexagonal phase occurs from the decomposed benzene-solvate (Dräger and Ross [12]). The X-ray diagrams during the decomposition are shown in Figure 5.

Vapor Pressures

In Fig. 6, $\log_{10}$ of the vapor pressures of hpdt · 2X in their dependence on 1/T are plotted. From the slopes of the straight lines the heats of vaporization ΔH_v are determined for each inclusion compound and listed in Table 6. For comparison, the ΔH_v of the free solvents are also given (from references [13–16]), likewise the straight lines $\log_{10} p(T)$ resulting from equations.

^2H NMR

The ^{2}H NMR measurements of the title compounds **1**, **2**, and **5** prove that the encaptured solvent molecules rotate in the crystal lattice about their pseudo threefold axis. Observed ^{2}H NMR spectra at several temperatures in hpdt · 2X (X = C_6D_6, $C_6D_5CD_3$, $C_6H_5ND_2$) are shown in Figures 7–9. For hpdt · 2 C_6D_6 (Fig. 7) an almost constant line shape

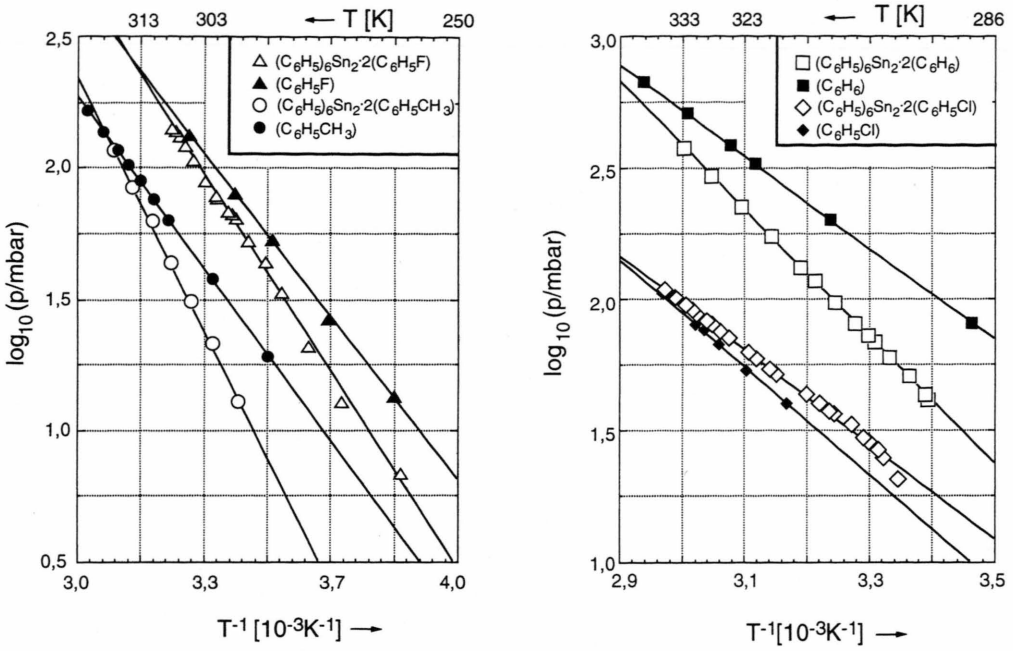

Fig. 6a, b. Plots of the vapor pressures ($\log_{10} p_{(T)}$) of the compounds hpdt · 2X, and the related free solvents.

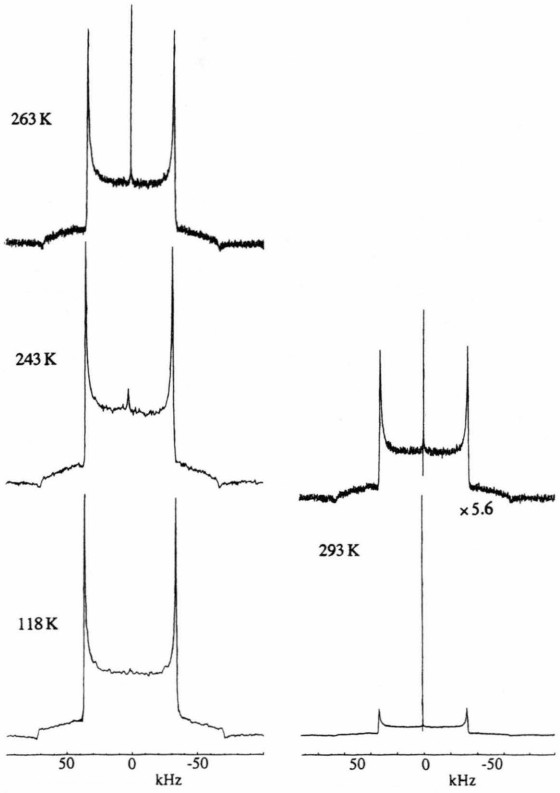

consisting of a Pake doublet was observed over the whole temperature range studied. The ^2H quadrupole coupling constant $e\Phi_{ZZ}Qh^{-1}$ (e = unit charge, Q = nuclear quadrupole moment, Φ_{ZZ} = main principal axis of the EFGT, h = Planck's constant) was evaluated from the observed peak separation $\Delta\nu$ given by $e\Phi_{ZZ}Qh^{-1} = (4/3)\,\Delta\nu$ under the assumption of a vanishing asymmetry parameter η ($\eta = |\Phi_{XX} - \Phi_{YY}|/|\Phi_{ZZ}|$) of the EFGT. $e\Phi_{ZZ}Qh^{-1}$ (^2H) values of 93.7 ± 0.5 and 87.3 ± 0.5 kHz were obtained at 118 and 293 K, respectively. Above ca. 240 K, a sharp central peak attributable to free C_6D_6 molecules was observed.

For hpdt · $2\,C_6D_5CD_3$ we observed two superimposed Pake patterns which showed a marked narrowing upon heating to room temperature. A pair of $e\Phi_{ZZ}Qh^{-1}$ values, 98 ± 2 and 47 ± 1 kHz, and 87 ± 2 and 22 ± 1 kHz were determined at 133 and 295 K, respectively. The spectra of the lattice-included perdeuterotoluene are shown in Figure 8. In Fig. 10

Fig. 7. Records of the ^2H NMR spectra of hpdt · $2\,C_6D_6$ at several temperatures. Above ca. 240 K a sharp single ^2H NMR peak of free (liquid, adsorbed) C_6D_6 appears as a singulet.

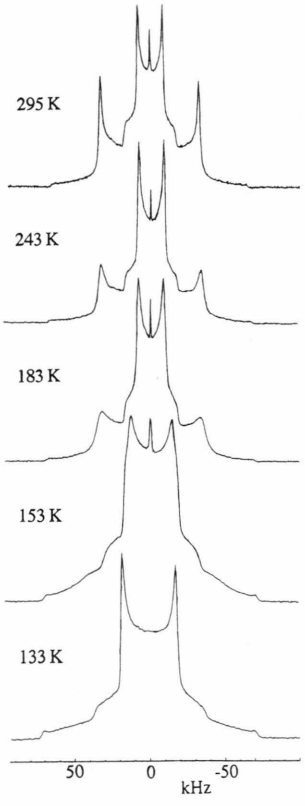

Fig. 8. Records of the ^2H NMR spectra of hpdt · $2C_6D_5CD_3$ as a function of temperature.

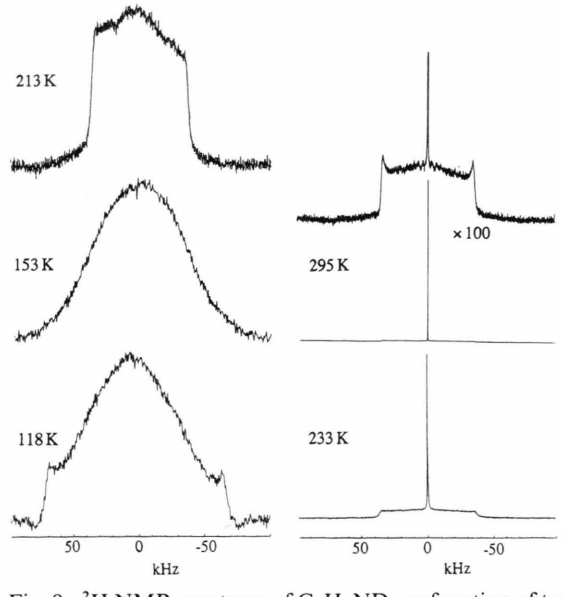

Fig. 9. ^2H NMR spectrum of $C_6H_5ND_2$ as function of temperature.

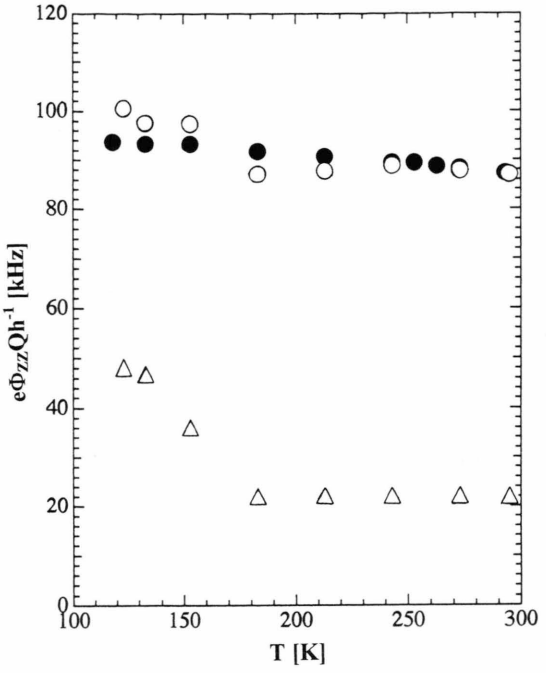

Fig. 10. Nuclear quadrupole coupling constants $e\Phi_{zz}Qh^{-1}$ of hpdt · $2C_6D_6$ [●] and hpdt · $2C_6D_5CD_3$ [○: C_6D_5, Δ: CD_3] as function of temperature

we show graphically the nuclear quadrupole constants of hpdt · $2C_6D_6$ and hpdt · $2C_6D_5CD_3$ in their dependence on temperature.

In hpdt · $2C_6H_5ND_2$, broad ^2H spectra were observed in the whole temperature range studied, as shown in Figure 9. From the observed $\Delta\nu$, we could determine $e\Phi_{zz}Qh^{-1}$ values of 176 ± 5 and 91 ± 2 kHZ at 118 and 295 K, respectively. Above ca. 220 K, a narrow central peak appeared in the presence of the broad Pake doublet, and the intensity of the sharp component increased with temperature.

Discussion

Crystal Structures

In hpdt · 2to, the phenyl ring is slightly distorted; especially the angle C(6)–C(1)–C(2), at the carbon atom bond to tin, deviates considerably from the ideal angle of 120°, being 117.5(4)°. The other angles vary from 119.0(5)° to 121.5(4)°; the C–C-bond lengths are 134.4(8) to 140.2(7) pm, the average being 137.8(7) pm. Such a deviation of the phenyl ring from ideal hexag-

onal symmetry is observed also in other compounds, where the phenyl ring is bond to a metal atom [17]. Due to its rotational motion, the toluene molecule is distorted, too. The bond lengths in the ring were fixed at 139 pm, and the bond C(8)–C(9) at 154 pm; the inner angles in the toluene ring are much strained, being 100(2)° and 140(2)°. Without constraints for the solvent molecule the bond lengths C(7)–C(8) are, alternating, 135(2) and 139(2) pm. The distance C(8)–C(9) is dynamically extremely shortened, being 124(4) pm. Such a rotational disorder was observed by Hönle et al. [18] in hexaphenyldisiloxane · 2toluene, where the bond lengths of the toluene ring are 124 and 149 pm, and the bond C(8)–C(9) is also very short with 122 pm. This solvate crystallizes in the same space group, $R\bar{3}$, with similar lattice constants like the compounds hpdt · 2X. The thermal parameters of the carbon atoms of the toluene molecule are also affected by its disorder, they are quite large compared to those of the carbon atoms of the phenyl ring in hpdt (more than twice as large!). The carbon atom C(9) of the methyl group of toluene could be refined only with isotropic thermal parameters; due to the threefold axis it occupies three different positions, related by symmetry, with a site occupancy of 1/3.

Many other solvates are known that are formed by molecules with similar shape like hpdt with aromatic solvents (hexaphenyldigermane · 2 benzene [2], triphenylmethane · X [19]). The host molecules are always aligned along an axis (Sn–Sn, Si–O–Si, C–H · · H–C), with large substituents on each side. This structural feature was already described by Toda et al. [3] and by Hart et al. [4]. Surprisingly, the solvent molecules are located between the "spacers", the phenyl rings, of two neighbouring host molecules and not edge-on to the long axis. Taking into account a distance from the midpoint of the toluene ring to a Sn-atom in hpdt · 2to of 508.7 pm, there can be no interaction between the metal atom and the π-system of the aromatic solvent. We assume that the formation of hpdt-solvates (and similar shaped molecules) follows the principle of optimum space filling within the crystal lattice, with van der Waals interaction between the different molecules. The interatomic distances (Table 3) lie in the range of van der Waals distances and support this assumption.

Of all title compounds, only hpdt · 2be has the molecular symmetry $\bar{3}$. Therefore, the results from X-ray powder diffraction are astonishing, because even the solvates formed with asymmetrical solvent molecules crystallize in $R\bar{3}$. But this can easily be explained by the disorder of the solvent molecules in the crystal lattice, they rotate about the normal of their ring planes, producing a pseudo threefold axis. Due to this disorder, they obey the high symmetry afforded by the space group $R\bar{3}$. So, because of the dynamic disorder in hpdt · 2to, the toluene molecule adopts the shape of mesitylene.

Table 7. Volume contraction $\Delta V/[10^{-6} \cdot \mathrm{pm}^3]$ of the solvent molecule X in the compound hpdt · 2X, compared to its volume V_{solv} in the pure crystalline form. V_{EZ}/Z is the volume of the formula unit in hpdt and hpdt · 2X, respectively.

Compound	V_{EZ}/Z $10^{-6} \cdot \mathrm{pm}^3$	V_{solv} $10^{-6} \cdot \mathrm{pm}^3$	ΔV $10^{-6} \cdot \mathrm{pm}^3$	Lit.
hpdt	771			[11]
hpdt · 2an	1043.83	136.42		this paper
an (252 K)		131.74	4.68	[20]
hpdt · 2be	1035.74	132.37		this paper
be (218 K)		122.92	9.45	[21]
hpdt · 2cb	1062.45	145.73		this paper
cb (120 K)		138.98	6.75	[22]
hpdt · 2fb	1040.40	134.70		this paper
hpdt · 2to	1068.78	148.89		this paper
to (165 K)		145.13	3.76	[23]

In Table 7 we have compared the free volume, available for the solvent molecule X in the compound hpdt · 2X, with the volume which X occupies in its pure solid crystallized form [20–23]. It is interesting to note that the solvent molecules in crystalline hpdt · 2X have a larger free volume available than in the pure crystalline solvent, and the "expansion" is around 2–5%. The effect should be mainly due to the higher excited librational spectrum in the solvate crystal compared to the pure crystalline solvent.

^2H-NMR

In the rigid lattice of C_6D_6, $e\Phi_{ZZ}Qh^{-1}$ (^{2}H) of 193 kHz and $\eta \approx 0$ has been reported by Rowell et al. [24]. In case a C_6D_6 rotates about an axis making an angle φ with the C–D bond direction, the nuclear quadrupole constant of ^{2}H decreases (Jelinski [25]) by $\frac{1}{2}(3\cos^2\varphi - 1)$ when $\eta = 0$. If the C_6D_6 molecule rotates about its C_6 axis, all six deuteron nuclei have the same $e\Phi_{ZZ}Qh^{-1}$ values, and the new value in the rotating molecule becomes half of the rigid value. The $e\Phi_{ZZ}Qh^{-1}$ (^{2}H) of 93.7 kHz observed in hpdt · $2C_6D_6$ at 118 K is accordingly, explained well by this model of rotation, indicating that all C_6D_6 molecules in the solid rotate frequently by more than 10^5 Hz in

this compound even at 118 K. With increasing temperature the line shape showed almost no change, but $e\Phi_{zz}Qh^{-1}$ (^{2}H) exhibited a gradual decrease which is attributable to thermal vibrations, and hence no new molecular motion is expected up to room temperature. The increase of the sharp peak observed above 240 K implies that the desolvation gradually progresses from about this temperature.

In hpdt · $2C_6D_5CD_3$ two kinds of Pake doublets with large and small splittings of roughly 2:1 intensity ratio were observed in the whole temperature range studied. The sharp and broad components could be assigned to CD_3- and phenyl-deuterium, respectively. Upon cooling from room temperature, both splittings became broad below 180 K and, even at the lowest temperature (123 K), the $e\Phi_{zz}Qh^{-1}$ (^{2}H) values seem to increase with decreasing temperature, as can be seen in Figure 8. By referring to the rigid lattice $e\Phi_{zz}Qh^{-1}$ value in C_6D_6 (193 kHz), the observed value of 175 kHz at 123 K implies the presence of almost rigid $C_6D_5CD_3$ molecules in the crystals. On the other hand, the CD_3 value of $e\Phi_{zz}Qh^{-1}$ of 47 kHz observed at 123 K is much smaller than the reported value of 165 kHz in the rigid lattice of $C_6D_5CD_3$ [24]. By applying Jelinski's term $\frac{1}{2}(3\cos^2\phi - 1)$, the CD_3 group rotation about the C_3 axis causes the static value to collapse by a factor of 1/3, namely, we obtain ca. 55 kHz for the C_3-rotating CD_3 group by assuming the tetrahedral bond angles in the CD_3 group. Since this value is close to the observed 47 kHz, the $C_6C_5CD_3$ molecules at 123 K can be characterized by almost a rigid phenyl ring and CD_3 rotation around C_3. Upon heating from 123 K, the two kinds of spectra were narrowed in around the same temperature range 130–180 K, indicating the onset of a new motion. Almost the constant $e\Phi_{zz}Qh^{-1}$ (^{2}H) values of 87 ± 2 and 23 ± 2 kHz observed above 180 K up to room temperature are just half of the respective low temperature values. Applying the same analysis used for the C_6D_6 compound, these results can be explained by the phenyl ring rotation about the axis perpendicular to the ring plane. This motional model agrees well with the results of the single crystal structure analysis given above. The sharp central peak observed at high temperatures was much weaker than in hpdt · $2C_6D_6$; this is consistent with the present experimental results of the vapor pressure measurements, that C_6H_6 showed a much higher vapor pressure than $C_6H_5CH_3$ in the protonated analogues.

In hpdt · $2C_6H_5ND_2$ we observed two outer peaks at 118 K separated by 132 ± 5 kHz, corresponding to $e\Phi_{zz}Qh^{-1}$ (^{2}H) of 176 ± 7 kHz by assuming $\eta=0$. The presence of a broad central component observed above this temperature indicates that some motion, which causes motional narrowing, is in progress in this temperature range. The lack of any structures in the spectra suggests the onset of superimposed different kinds of motions, e.g. two or three site jumps of ^{2}H nuclei among nonequivalent sites. Since the static nuclear quadrupole coupling constant (^{14}N) in amido ND_2 groups has been reported in a range of 190–200 kHz (Edmonds [26]), the observed 176 kHz at 118 K implies that $C_6H_5ND_2$ molecules are almost rigid at this temperature. The sharp central peak observed upon heating to above 200 K can be attributed to the liberation of free aniline molecules. Around room temperature, we observed a broad component with an almost temperature independent line width. The $e\Phi_{zz}Qh^{-1}$ (^{2}H) value of 91 ± 2 kHz obtained at 295 K became roughly half of the low-temperature value. This indicates the excitation of the inplane rotation of $C_6H_5ND_2$ molecules analogous to the above mentioned C_6D_6 and $C_6H_5CD_3$ motion, and the absence of the C_2 rotation or the hydrogen exchange in the ND_2 group.

Vapor Pressures

The vapor pressures of the title compounds should give some hint about their stability and possible interactions of the molecules within the crystal lattices. For the compounds hpdt · 2be, hpdt · 2fb and hpdt · 2to, the vapor pressures are lower than those of the corresponding pure solvents (liquid state). We conclude that the interactions between the host and guest molecules in the crystal lattices are slightly stronger than the interactions between the solvent molecules in pure liquid form. For hpdt · 2cb, a higher vapor pressure is determined, compared to pure chlorobenzene, the difference being small. This can be explained with stronger dipole interactions in liquid chlorobenzene, while in the solvate the guest molecules are isolated from each other and the interactions between hpdt and chlorobenzene are dominated by van der Waals forces.

Very interesting is the behaviour of hpdt · 2an. Here, within the limits of error, the same vapor pressure as for pure aniline is measured. We assume that the encaptured aniline evaporates out of the crystal

solvate, and as soon as a few aniline molecules reach the crystal surface, they stick together by hydrogen bonds, forming a film of pure liquid aniline above the crystallites. Therefore, the vapor pressure of free aniline is measured. To find out the real vapor pressure of aniline above the crystalline solvate, a dynamical method for the measurement of $p = f_{(T)}$ has to be used. It is quite likely that, because of the missing hydrogen bonds N–H · · · N in the crystal solvate, the vapor pressure of hpdt · 2an is higher than that of pure aniline at the corresponding temperature.

Acknowledgement

We are grateful to the "Deutsche Forschungsgemeinschaft" and the "Fonds der Chemie" for support of the work.

[1] E. Krause and R. Becker, Ber. Dtsch. Chem. Ges. **53,** 173 (1920).
[2] H. Piana, U. Kirchgäßner, and U. Schubert, Chem. Ber. **124,** 743 (1991).
[3] F. Toda, D. L. Ward, and H. Hart, Tetrahedron Lett. **22,** 3865 (1981).
[4] H. Hart, L. T. W. Lin, and D. L. Ward, J. Amer. Chem. Soc. **106,** 4043 (1984).
[5] E. Krause and A. Grosse, „Die Chemie der metall-organischen Verbindungen", Gebr. Borntträger, Berlin 1937 S. 361.
[6] G. M. Sheldrick, SHELXS86. Program for the solution of crystal structures, Univ. of Göttingen, Germany (1986). SHELXL93. Program for crystal structure determination, Univ. of Göttingen, Germany (1993).
[7] A. Smith and A. W. C. Menzies, Ann. d. Phys. (4) **33,** 971 (1910); Z. Phys. Chem. **75,** 501 (1911).
[8] R. Strauss, Dissertation, Darmstadt (1995).
[9] J. H. Davis, K. P. Jeffrey, M. Bloom, M. F. Valic, and T. P. Higgs, Chem. Phys. Lett. **42,** 390 (1976).
[10] E. Sternin, M. Bloom, and A. L. MacKay, J. Magn. Reson. **55,** 274 (1983).
[11] H. Preut, H.-J. Haupt, and F. Huber, Z. anorg. allg. Chem. **396,** 81 (1973).
[12] M. Dräger and L. Ross, Z. anorg. allg. Chem. **469,** 115 (1980).
[13] J. Timmermans, Physico-chemical constants of pure Org. compounds, Elsevier, Amsterdam 1950.
[14] J. M. Stuckey and J. H. Saylor, J. Amer. Chem. Soc. **62,** 2922 (1940).
[15] R. Dreyer, W. Martin, and U. von Weber, J. prakt. Chem. **1,** 324 (1955).
[16] R. R. Dreisbach and S. A. Shrader, Ind. Eng. Chem. **41,** 2879 (1949).
[17] M. R. Churchill and T. A. O'Brien, J. Chem. Soc. A **1969,** 266.
[18] W. Hönle, V. Manriquez, and H. G. von Schnering, Acta Cryst. **C46,** 1982 (1990).
[19] A. Allemand and R. Gerdil, Acta Cryst. **A31,** 130 (1975).
[20] M. Fukuyo, K. Hirotsu, and T. Higuchi, Acta Cryst. **B38,** 640 (1982).
[21] G. E. Bacon, N. A. Curry, and S. A. Wilson, Proc. Roy. Soc. London **A279,** 98 (1964).
[22] D. Andre, R. Fourme, and M. Renaud, Acta Cryst. **B27,** 2371 (1971).
[23] M. Anderson, L. Bolio, J. Bruneaux-Poulle, and R. Fourme, J. Chim. Phys. **74,** 68 (1977).
[24] J. C. Rowell, W. D. Phillips, L. R. Melby, and M. Panar, J. Chem. Phys. **43,** 3442 (1965).
[25] L. W. Jelinski, Ann. Rev. Mater. Sci. **15,** 359 (1985).
[26] D. T. Edmonds, Phys. Rep. **29,** 233 (1977).